Site-Directed Mutagenesis of Histidine 245 in Firefly Luciferase: A Proposed Model of the Active Site†

Bruce R. Branchini,* Rachelle A. Magyar, Martha H. Murtiashaw, Shannon M. Anderson, and Marc Zimmer

Department of Chemistry, Connecticut College, 270 Mohegan Avenue, New London, Connecticut 06320

Received May 18, 1998; Revised Manuscript Received July 30, 1998

ABSTRACT: Firefly luciferase catalyzes the highly efficient emission of yellow-green light from substrate luciferin by a sequence of reactions that require Mg-ATP and molecular oxygen. We previously reported [Branchini, B. R., Magyar, R. A., Marcantonio, K. M., Newberry, K. J., Stroh, J. G., Hinz, L. K., and Murtiashaw, M. H. (1997) *J. Biol. Chem. 272*, 19359−19364] that 2-(4-benzoylphenyl)thiazole-4-carboxylic acid (BPTC), a firefly luciferin analogue, was a potent photoinactivation reagent for luciferase. We identified a luciferase peptide 244HHGF247, the degradation of which was directly correlated to the photooxidation process. We report here the construction and purification of wild-type and mutant luciferases H244F, H245F, H245A, and H245D. The results of photoinactivation and kinetic and bioluminescence studies with these proteins are consistent with His245 being the primary functional target of BPTC-catalyzed enzyme inactivation. The possibility that His245 is oxidized to aspartate during the photooxidation reaction was supported by the extremely low specific activity (∼300-fold lower than WT) of the H245D mutant. Using the crystal structures of luciferase without substrates [Conti, E., Franks, N. P., and Brick, P. (1996) *Structure 4*, 287−298] and the functionally related phenylalanine-activating subunit of gramicidin synthetase 1 [Conti, E., Stachelhaus, T., Marahiel, M. A., and Brick, P. (1997) *EMBO J. 16*, 4174−4183] as a starting point, we have performed molecular-modeling studies and propose here a model for the luciferase active site with substrates luciferin and Mg-ATP bound. We have used this model to provide a structure-based interpretation of the role of 244HHGF247 in firefly bioluminescence.

Bioluminescence is a fascinating process in which living organisms convert chemical energy into light. Beetle bioluminescence, observed in perhaps 2000 species of fireflies (*1*, *2*), has provided a fruitful area of basic and applied research mainly focused on the North American firefly *Photinus pyralis* (*3*). In this firefly species, the luciferase-catalyzed light emission process is extremely efficient; in alkaline solution, nearly a single photon is emitted per reacted luciferin molecule (*4*). The enzyme luciferase functions as a monooxygenase, without the apparent involvement of a metal or cofactor (Figure 1). According to the enzymatic mechanism (*5*, *6*) presented in Figure 1, the beetle luciferases catalyze a sequence of reactions that convert firefly luciferin into an electronically excited state oxyluciferin product which then emits light. First, luciferase catalyzes the formation of an enzyme-bound luciferyl adenylate (Figure 1, step a). Next, a proton is abstracted from the C-4 carbon of the adenylate by a presumed luciferase base (step b); molecular oxygen adds to the newly formed anion (step c); and an electronically excited-state oxyluciferin molecule and CO_2 are produced from a highly reactive dioxetanone intermediate (steps d and e). According to the original theory (*5*, *6*) based predominantly on studies of the *P. pyralis* enzyme, red light emission (λ_{max} 615 nm), which is observed at pH 6.0, results from the keto form of the emitter. At pH 7.8, the familiar yellow-green light emission (λ_{max} 560 nm) is produced from the enolate dianion form of the excited-state oxyluciferin by a presumed enzymatic assisted tautomerization (step f). In nature, beetle luciferases display various colors of light from green (λ_{max} ∼540 nm) to red (λ_{max} ∼635 nm) (*7*, *8*). On the basis of results of molecular orbital calculations, McCapra has proposed (*9*, *10*) that red bioluminescence is generated from a twisted charge-transfer excited state of the keto form of oxyluciferin. It has been suggested (*9*, *10*) that changes in luciferase tertiary structure might modulate color by affecting the stabilization of oxyluciferin conformers formed by rotation about the C2−C2′ bond. The proposed mechanisms for bioluminescent color recently have been reviewed (*9*−*11*).

Luciferase also catalyzes the in vitro formation of the adenylate of dehydroluciferin, which cannot react further. This adenylate may be produced by oxidation of enzyme-bound luciferyl−AMP (*12*). Luciferase can also function as a ligase (*13*) as the AMP group of the enzyme luciferyl−AMP complex can be transferred to ATP to produce diadenosine tetraphosphate.

The luciferase-catalyzed reactions provide the basis for a wide variety of biochemical assays, many with important clinical applications (*14*−*16*). Moreover, the luciferase gene (*17*) is widely used as a reporter in studies of gene expression and regulation (*18*), including real-time monitoring in living mammals (*19*). Additionally, the cloning and sequencing of *P. pyralis* luciferase (Lase)[1] and homologues from several

† This work was supported by the McCollum-Vahlteich Endowment. Portions of this work were presented at the 215th National Meeting of the American Chemical Society, Dallas, Texas, March, 1998.

* To whom correspondence should be addressed. Tel: (860) 439-2479. Fax: (860) 439-2477. E-mail: brbra@conncoll.edu.

10.1021/bi981150d CCC: $15.00 © 1998 American Chemical Society
Published on Web 10/14/1998

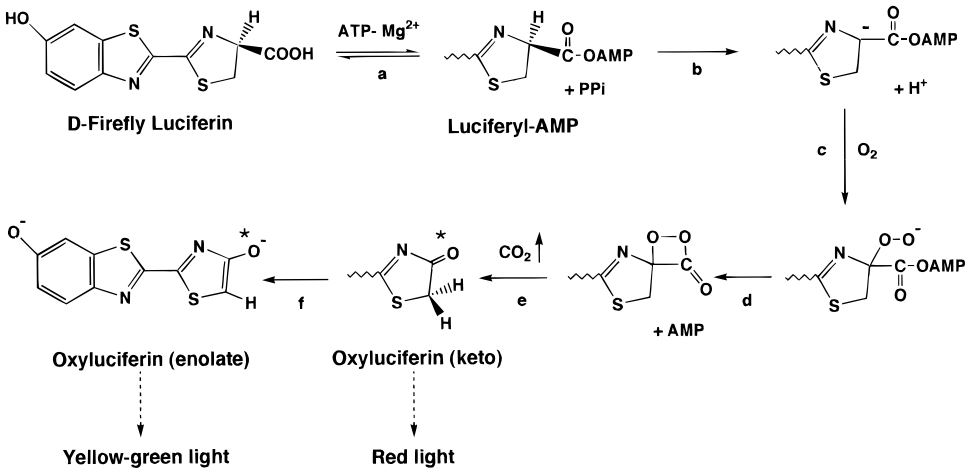

FIGURE 1: Mechanism of firefly luciferase catalyzed bioluminescence.

beetles (*11*, *20*) have revealed that these enzymes are closely related to a large family of nonbioluminescent proteins (*21*, *22*) which catalyze reactions of ATP with carboxylate substrates to form acyl adenylates. This group of proteins, which share an identifying motif (198SSGSTGLPKG207 in Lase), has recently been termed the "acyl-adenylate/thioester-forming" enzyme family (*23*).

Mutational studies of the luciferases have been conducted including several (*11*, *24*−*29*) that have identified changes in single and/or groups of amino acids widely distributed throughout the sequences of nine luciferases which affect the color of bioluminescence. The comparative studies of these luciferase sequences from five firefly species—*Hotaria parvula* (*26*), *Pyrocoelia miyako* (*26*), *Luciola cruciata* (*25*), *Luciola mingrelica* (*27*, *28*), and *P. pyralis* (*24*)—and the four click beetle [*Pyrophorus plagiophthalamus* (*11*, *29*)] isozymes have not yielded any direct structure−function relationship to account for the color variation of firefly bioluminescence. The Lase thiols, originally believed to be important for catalysis, have been shown to be nonessential (*30*−*34*). Random and saturated mutagenesis studies (*35*, *36*) of *L. cruciata* and *P. pyralis* luciferases have produced thermostable mutants, T217I and E354K/E354R, respectively. We recently reported (*37*) mutational studies of Lase that demonstrated Ser198 directly influences the K_m of substrate Mg-ATP, the overall pK_a of bioluminescence, and the emission decay kinetics. Our results and those reported with *L. mingrelica* (*32*) led us to suggest that the region Ala193−Val208, a highly conserved Lase domain common to the acyl-adenylate/thioester-forming enzyme family, is directly involved in Mg-ATP binding but not luciferin binding.

[1] Abbreviations: BPTC, 2-(4-benzoylphenyl)thiazole-4-carboxylic acid; buffer A, 0.1 M potassium phosphate, 1 mM EDTA, 0.8 M $(NH_4)_2SO_4$, 1% glycerol, and 1 mM β-mercaptoethanol, pH 7.8; CB (PreScission protease cleavage buffer), 50 mM Tris-HCl (pH 7.0), 150 mM NaCl, 1 mM EDTA, and 1 mM DTT; gly-gly, 25 mM glycyl-glycine, pH 7.8; GST, glutathione-*S*-transferase; IPTG, isopropyl-β-D-thiogalactoside; Lase, *Photinus pyralis* luciferase (EC 1.13.12.7); LB, Luria−Bertani growth media; LC/ESMS, tandem HPLC-electrospray ionization mass spectrometry; MC, Monte Carlo; NaPB, 0.1 M sodium phosphate buffer (pH 8.0); PheA, the phenylalanine-activating subunit of gramicidin synthetase 1; RLU, relative light unit; SDS−PAGE, sodium dodecyl sulfate−polyacrylamide gel electrophoresis; WT, wild-type *Photinus pyralis* luciferase containing the additional N-terminal peptide GPLGS.

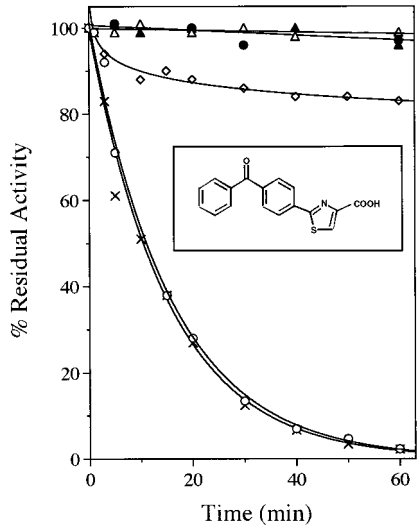

FIGURE 2: Photoinactivation of luciferases by BPTC. WT (×), H244F (○), and H245F (◇) luciferases (8 μM in NaPB) were irradiated in the presence of 4 μM BPTC under the standard irradiation conditions described previously (*39*). Aliquots (4 μL) were withdrawn from the incubations at the indicated times and analyzed for enzyme activity. Control studies were performed by irradiating WT (△), H244F (▲), and H245F (●) under identical conditions in the absence of BPTC. The chemical structure of BPTC is shown in the inset.

Recently, the crystal structure of Lase without bound substrates or ligands was reported (*38*). The protein has a unique molecular architecture consisting of a large N-terminal domain (residues 1−436) and a small C-terminal domain (residues 440−550). The general location of the active site was proposed after analysis of the positions of seven absolutely conserved residues among approximately 40 enzymes sharing the adenylation function. Many of these invariant residues were found on the surfaces of the two Lase domains opposite to each other and separated by a wide solvent filled cleft. However, the exact locations of the substrate binding sites were not established (*38*).

Previously, we reported (*39*) that 2-(4-benzoylphenyl)-thiazole-4-carboxylic acid (BPTC, Figure 2, inset) was a potent photoinactivation reagent for Lase. We identified a chymotryptic peptide, 244HHGF247, the degradation of which was directly correlated to Lase photoinactivation. We subsequently have undertaken a mutational analysis of the peptide to better understand its role in firefly biolumines-

Table 1: Bioluminescence Activity of Luciferase Enzymes[a]

enzyme	relative specific activity[b] flash height (RLU s^{-1}/mg)	integrated (RLU/mg)	rise time[c] (s ± 0.15)	decay time[d] (min ± 0.1)
WT	100	100	0.5 (0.4)	0.2
H245D[e]	0.3	2.6	59.2 (9.9)	11.7
H245A	22.0	80	0.9 (0.8)	0.9
H245F[f]	4.2	21	1.5 (0.4)	0.8
H244F	18.4	48	1.0 (nd)	1.6

[a] Activity measurements were made in gly-gly buffer as described (*37*) except that the amount of luciferin in the standard assays was 70 μM. [b] WT values are defined as 100 and are equivalent to 118 RLU s^{-1}/mg and 2450 RLU/mg for flash height-based and 15 min integration-based assays, respectively. These data were corrected for the spectral response of the Hamamatsu 931B photomultiplier tube used in the assays. Bioluminescence emission maxima were: WT (560 nm), H245D (617 nm), H245A (608 nm), H245F (576 nm), and H244F (560 nm). [c] Values in parentheses were determined in 400 μL of 50 mM glycylglycine buffer (pH 7.8) and 4 μg of luciferase. Assays were initiated by injection of 20 μL of 0.1 mM synthetic luciferin-AMP in 10 mM sodium acetate (pH 4.5). The final pH in these assays was 7.8. [d] Values represent the time interval from attainment of maximum flash height to 20% of this maximum emission intensity. [e] Substrate concentrations in the activity assays were 4 mM Mg-ATP and 150 μM luciferin. [f] Substrate concentrations in the activity assays were 3 mM Mg-ATP and 180 μM luciferin.

cence. During the course of our studies, the crystal structure of a second member of the superfamily, the phenylalanine-activating subunit of gramicidin synthetase 1 (PheA) in a complex with Phe, Mg ion, and AMP, was reported (*40*). Using the Lase coordinates (*38*) and a description of the PheA complex (*40*) as a starting point, we have performed molecular modeling studies designed to produce a model of the Lase active site containing substrates luciferin and Mg-ATP. We present this model here and use it to interpret the results of mutational studies of 244HHGF247.

MATERIALS AND METHODS

Materials. *P. pyralis* cDNA in the vector pSx(T7)-Ppy was a generous gift of Monika Gruber. The following items were obtained from the indicated sources: Mg-ATP (equine muscle) (Sigma); luciferin (Biosynth AG); Luria-Bertani (LB) growth media components (Difco); restriction endonucleases, T4 polynucleotide kinase and T4 DNA ligase (New England Biolabs); mutagenic oligonucleotides (Genosys); *Escherichia coli* strain DH5αF′IQ (Gibco BRL); Altered Sites II in vitro mutagenesis kit and *E. coli* strains BMH71−18*mutS*, JM109 (DE3), and JM109 (Promega); Bulk GST Purification Module, pGex-6p-2 expression vector and PreScission protease (Pharmacia Biotech); isopropyl-β-D-thiogalactoside (IPTG) (Boehringer Mannheim); and Slide-A-Lyzer (10K) dialysis cassettes (Pierce).

General Methods. Luciferase bioluminescence activity was determined using flash height-based and integration-based light assays. The standard activity assays were performed in gly-gly buffer as described previously (*33*, *37*) with the exceptions noted in Table 1. To relate activity units (RLU s^{-1}/mg), to conventional flash height measurements, the number of photons emitted in a 0.5 s interval at the maximum peak height was recorded under the standard assay conditions. These measurements do not depend on the time (rise time) to reach maximum (peak) light intensity. One RLU is equivalent to 10^{13} photons (*41*). The integration-based assays were performed as described (*37*) except that coenzyme A was omitted and the integration time was 15 min. All light measurements were corrected for the spectral response of the Hamamatsu 931B photomultiplier tube used in the assays.

The following measurements were performed as previously described: time dependence of bioluminescence initiated with luciferin and Mg-ATP or synthetic luciferyl−AMP (*37*, *41*); corrected bioluminescence emission spectra (*41*); photoinactivation studies with BPTC (*39*); the effect of O_2 on light emission kinetics (*41*); and rise times to maximum bioluminescence intensity (*41*). All flash height measurements were made by injecting the initiating solutions with a Hamilton Microlab 900 automatic dispenser operated at the maximum speed. The estimated mixing time was ∼0.2 s. Data were acquired with a Strawberry Tree, Inc., A/D converter using a sampling rate of 0.05 s and a Macintosh SE computer.

Site-Directed Mutagenesis. Mutations at H244 and H245 were created by oligonucleotide-directed mutagenesis (*42*) using antibiotic selection with an Altered Sites II kit and the pSx(T7)-Ppy plasmid. Phagemid ssDNA templates were prepared by infection of DH5αF′IQ cells containing the pSx-(T7)-Ppy plasmid with helper phage R408. The following mutagenic primers were designed for annealing onto the ssDNA template: H245A, 5′-T TTA AGT GTG GTA CCA TTC CAT **GCC** GGT TTT GG-3′; H245D, 5′-T TTA AGT GTG GTA CCA TTC CAT **GAC** GGT TTT GG-3′; H245F, 5′-T TTA AGT GTG GTA CCA TTC CAT **TTC** GGT TTT GG-3′; H244F, 5′-T TTA AGT GTG GTA CCA TTC **TTT** CAC GGT TTT GG-3′ (underline represents silent changes to create a unique *Kpn*I site and the bold represents the mutated codon). The primer 5′-CAC ACA GTA GAC AGG ATC ATG GAA GAC G-3′ (underline represents a new *Acc*I site) was designed to align the Lase cDNA reading frame for subcloning into the pGex-6p-2 fusion vector and was included in each mutagenesis reaction.

Double-stranded DNA products synthesized with an Altered Sites II kit were transformed into a *mutS* strain of BMH71−18 and grown in ampicillin-containing LB. Plasmid minipreps were transformed into JM109(DE3) cells, and colonies grown on 0.2 μm nitrocellulose were screened by in vivo bioluminescence assays.[2] Putative mutant clones containing the *Acc*I and *Kpn*I sites were selected by restriction analysis. DNA inserts were isolated by digestion with *Bam*HI and *Xho*I and were subcloned directly into the expression vector pGex-6p-2. The entire cDNA of all luciferase genes was verified by DNA sequencing.

Expression and Purification of Luciferases. Glutathione-S-transferase (GST) fusion constructs, encoding wild-type (WT) and mutant fusion proteins, were expressed in *E. coli* JM109. Cultures (250 mL) were grown in 1 L flasks at 37 °C in LB medium supplemented with 100 μg/mL ampicillin to mid log phase (A_{600} = 0.6−0.9), induced with 0.1 mM IPTG, and incubated at 25 °C for 8−10 h. The cells were harvested by centrifugation at 4 °C and stored overnight at −70 °C. Cell pellets were resuspended in 50 mL of a solution of 140 mM NaCl, 2.7 mM KCl, 10 mM Na_2HPO_4, and 1.8 mM KH_2PO_4 (pH 7.3) containing 0.1 mM phenylmethanesulfonyl fluoride. Lysozyme (0.05 volume of 10 mg/

[2] Monika Gruber, Promega Corp. Madison, WI, personal communication.

mL) was added, and the cells were lysed by sonication. Triton X-100 (2% final volume) was added to the lysate and the whole-cell extract was isolated by centrifugation at 20000*g* for 1 h.

WT and luciferase mutant proteins were purified from whole-cell extracts using Glutathione Sepharose 4B affinity chromatography according to the manufacturer's instructions. Luciferases were released from fusion proteins by incubation with PreScission protease in PreScission protease cleavage buffer (CB) [50 mM Tris-HCl (pH 7.0), 150 mM NaCl, 1 mM EDTA, and 1 mM DTT] for 18−20 h at 5 °C. Proteins were eluted with CB and stored at 4 °C in CB containing 0.8 M ammonium sulfate and 2% glycerol.

Protein Analysis. Luciferase protein concentrations were determined by UV spectroscopy using $\epsilon_{278} = 45\,560\ M^{-1}\ cm^{-1}$ (*43*). For solutions containing DTT, the Bio-Rad protein assay was used with BSA as the standard. SDS−PAGE was performed according to the method of Laemmli (*44*), and gels were stained with Coomassie R-250.

Spectroscopy. Guanidinium-chloride-induced denaturation of the luciferases was monitored by fluorescence spectroscopy (*45*) using stock enzyme solutions (10 μg/mL) which had been dialyzed against 0.1 M potassium phosphate, 1 mM EDTA, 0.8 M $(NH_4)_2SO_4$, 1% glycerol, and 1 mM β-mercaptoethanol, pH 7.8 (buffer A). Fluorescence emission spectra (300−400 nm) were measured at 22 °C in quartz cells using a Perkin-Elmer LS-5B spectrometer. An excitation wavelength of 280 nm was used, and all spectra were corrected for fluorescence of buffers. Enzymes were incubated for 15 min with increasing concentrations of guanidinium chloride (1−6 M) in buffer A. The midpoint denaturant concentrations were determined graphically by comparison of fluorescence intensities at 335 nm.

Circular dichroism spectra of 0.3−0.4 mg/mL solutions of luciferases in buffer A were measured at 20 °C using a 0.1 mm path-length cell with a Jasco J-720 spectropolarimeter. Data points were taken from 180 to 240 nm at 0.2 nm intervals at a spectral bandwidth of 1 nm. Spectra were accumulated over four repeated scans and corrected for solvent background. Mean residue ellipticities were calculated using a mean residue weight of 110.2.

Kinetic Constants. Steady-state kinetic constants (*37*) were determined from activity assays (described above) in which measurements of maximum light intensity were made and taken as estimates of initial velocities. No correction was made for the differences in rise times to maximum intensity (Table 1). The concentration of one substrate was maintained at saturation, and the other was varied: 0.5−200 μM for luciferin and 0.02−2.5 mM for Mg-ATP. Kinetic constants were calculated by the method of nonlinear least squares using Enzfitter (Biosoft) software.

Molecular Modeling. The AMBER* force field as implemented in MacroModel version 6.0 (*46*) was used for all molecular modeling. It uses a 6,12 Lennard-Jones hydrogen-bonding treatment (*47*) and an improved protein backbone parameter set (*48*).

The Lase solid-state structure [1LCI (*38*)] obtained from the Protein Data Bank (*49*) provided the starting point for the computational study. Due to disorder, amino acids 199−203, 356−358, 436−440, and 524−528 were omitted from the crystal structure (*38*). The missing residues were drawn so that they bridged the gaps in the solid-state structure. The lowest energy conformations of these residues within the known Lase solid-state structure were determined by dihedral Monte Carlo (MC) multiple minimum searches (*50*). Each MC step varied between 1 and all the rotatable dihedral angles in the graphically placed residues by between 0 and 180°. Ring closure bonds were placed in the residues adjacent to the new residues. A minimum ring closure distance of 1.00 Å and a maximum of 4.00 Å were used. Structures within 50 kJ/mol of the lowest energy minimum were kept and a usage directed method (*51*) was used to select structures for subsequent MC steps. Three thousand MC steps were taken for each search. All conformations within 50 kJ/mol of the lowest energy conformation were combined and subjected to 10 000 iterations with the multiconformer minimization mode of MacroModel. All unique conformations within 50 kJ/mol of the global minimum structure were kept. A "hot" sphere of 12 Å from the disordered residues, with a secondary constrained sphere extending further by 3 Å, was used in all conformational searches. Constraints were introduced with a harmonic restoring potential of 100 kJ/Å^2. The side chains of 31 residues were not located in the solid-state structure of Lase (*38*). Since Leu204, Lys321, Glu322 and Lys529 were within 15 Å of the putative active site, their side chains were drawn and minimized within the lowest energy conformation of the 1LCI solid-state structure determined as described above. Preminimized luciferyl−AMP was placed in the active site of the modified structure, solvent molecules were removed, and the complex was minimized. A dihedral MC multiple minimum search, in which all variable dihedral angles within the luciferyl−AMP were randomly varied, was carried out, as described above, to find the lowest energy conformation within the enzyme. The movement of the substrate was restrained by the addition of three short restraints (two between the 6′-oxygen anion of luciferin and two of the side-chain R218 NHs, and one between an adenine N6 amino proton and the G339 main chain carbonyl oxygen) and three long restraints (between the two ribose hydroxyl group protons to the carboxylate of D422, and between the other adenine N6 amino proton and the N338 side chain carbonyl oxygen). Flat-bottom energetic restraint wells were used with force constants of 100 kJ/Å^2 for the long restraints and 200 kJ/Å^2 for the short ones. A desired distance of 2.5 Å with a half-width of the flat bottom of 1.5 Å was used for the short restraints, and an ideal distance of 3.0 Å with a half-width of 2.0 Å was used for the long restraints. A "hot" sphere of 10 Å from the luciferyl−AMP, which was enlarged to include residues 198−206, with a secondary constrained sphere extending further by 3 Å, was used in the conformational search.

Eighty-one structures were obtained with an energy within 50 kJ/mol of the lowest energy structure. Conformational families of the luciferyl−AMP within Lase were established with the agglomerative, hierarchical single-link clustering program, Xcluster (*52*).

The lowest energy conformation of luciferyl−AMP in Lase was graphically converted to the luciferin, ATP, and Mg^{2+} complex. Methylammonium ion was included in the complex to mimic any interactions of the K529 side chain with the substrates that would not be allowed by the limitations of the size of the searched conformational space. The AMBER* parameters were supplemented by the addition

of the Mg^{2+} parameters used to model magnesium coordination to cyclohexane-1,2,3-triol triphosphates (*53*). The complex was minimized and a dihedral MC multiple minimum search (1000 steps) was performed in which all variable dihedral angles within luciferin and ATP were varied. The conditions were identical to those for the luciferyl−AMP search except that only the three short restraints were used. The lowest energy conformation was subjected to an additional random 1000 rotational and/or translational steps of the luciferin, ATP, and Mg^{2+} within the Lase. The luciferin and ATP were rotated by between 0 and 180°, and the luciferin, ATP, and Mg^{2+} were translated by between 0 and 3 Å in each MC step with the three short restraints in place. Finally, the lowest energy binding geometry obtained in this manner was subject to 2000 steps of a dihedral, rotational, and translational MC multiple minimum search. Low-energy conformations were collected and clustered as described above.

RESULTS AND DISCUSSION

Overexpression, Purification, and Characterization of Luciferase Proteins. WT and mutant luciferases listed in Table 1 were expressed as GST-fusion proteins, which, after protease cleavage, contained the additional N-terminal peptide GPLGS. Proteins were purified to homogeneity (as judged by SDS−PAGE) in yields of 8−14 mg/L culture volume. All enzymes maintained full activity for at least 3 months when stored at 4 °C in CB containing 0.8 M ammonium sulfate and 2% glycerol.

Mutations at position 245 had little, if any, effect on secondary structure as the far-UV circular dichroic (CD) spectra (data not shown) of the mutants and WT were nearly indistinguishable; all spectra had minima at 208 and 222 nm, $\theta = -7840$ and -7680 deg dm^{-1} nM^{-1}, respectively. Attempts to measure near-UV CD spectra of the luciferases, however, were unsuccessful. The tertiary structure and thermodynamic stability of the mutants appear to be very similar to those of WT, as judged by superimposable fluorescence emission spectra and identical guanidinium chloride-induced denaturation curves with midpoint denaturant concentration equal to 3.5 M ± 0.3 (data not shown).

Photoinactivation Studies with BPTC. We previously reported (*39*) that the novel substrate analogue BPTC, a potent reversible competitive inhibitor ($K_i = 3.0 \pm 0.3$ μM) with respect to luciferin ($K_m = 15 \pm 2.0$ μM), inactivated Lase by a photooxidation process involving singlet oxygen. The inhibition was correlated with the loss of the chymotryptic peptide 244HHGF247 which was the predominant, but not the sole, site of photoinactivation. Since His244 and/or His245 are potential sites of photooxidation, we constructed single point mutants with Phe substituted at either site to determine the role of these His residues in Lase inactivation. The His → Phe substitution was chosen because the Phe side-chain aromatic group is resistant to photooxidation. Additionally, while all known luciferase sequences have His at position 245, Phe is found at position 244 (*P. pyralis* numbering) in the four click beetle enzymes (*11, 20, 29*). Mutant H244F was inactivated by photolysis with BPTC in a nearly identical manner to the WT (Figure 2). In contrast, the H245F mutant initially lost ∼17% activity and was resistant to further inactivation. Since photoinactivation required His at position 245 and not at 244, we focused further studies on the role of invariant His245 in luciferase bioluminescence.

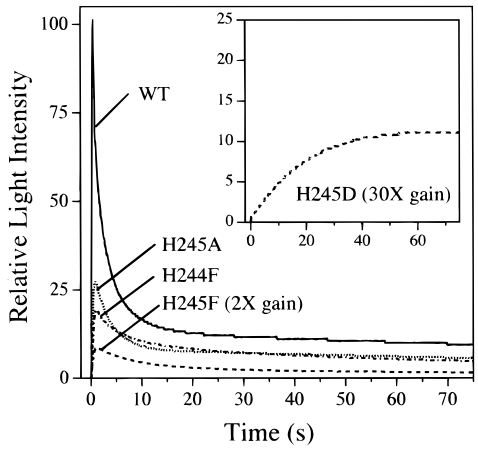

FIGURE 3: Light emission kinetic profiles. Light emission data from standard bioluminescence activity assays of luciferases performed as described in the Materials and Methods with the exceptions noted in the Table 1 legend were recorded at pH 7.8.

Bioluminescence Activity of the Luciferases. We expressed, purified, and characterized two additional mutant proteins, H245A and H245D. The alanine mutant was chosen to enable us to evaluate the functional role of the imidazole group of His245. The H245D mutant was intended to represent a possible protein product of BPTC-catalyzed photooxidation of Lase. Previously, we presented (*39*) LC/ESMS evidence from a model BPTC photooxidation study with the synthetic peptide HHGF which indicated that the histidine residues were converted into aspartic acid and peroxide adducts. Although His244 may also be photooxidized, the results (Figure 2) discussed above indicated that this residue was not associated with the photoinactivation process.

Specific activities for all luciferases were measured and expressed as flash height (RLU s^{-1}/mg)- or integration (RLU/mg)-based values (Table 1). The former measurements, as defined in the Materials and Methods, relate the maximum achievable overall reaction rate for all steps shown in Figure 1. These specific activity values are useful for making comparisons of the WT and mutant properties; however, these measurements do not take into account the time it takes each enzyme to achieve its maximum output (i.e., rise time). Also, the flash height-based specific activities are independent of the duration that the maximum rate is sustained. The time dependence of bioluminescence intensity of the luciferases did vary, and these data are presented in Table 1 and Figure 3. Mutants H245A, H245F, and H244F had moderately prolonged emission profiles compared to WT. The rise time to maximal peak height for H245D reactions was ∼100 times slower than WT, and the subsequent decay was ∼60 times longer.

The flash height-based specific activity of the Asp mutant was ∼300-fold lower than WT, whereas the specific activities of the H245A, H244F, and H245F mutants were reduced ∼4.5-, ∼5.5-, and ∼24-fold, respectively. The bioluminescence activity of H245D is approximately equivalent to >99% inactivated Lase. The very low activity of the Asp mutant and the supporting model study results (*39*) suggest that His245 may be oxidized to aspartate as a consequence

of BPTC irradiation of Lase. However, the inactivation of Lase by histidine peroxide formation during the photoinactivation process cannot be discounted. The specific activities of the two phenylalanine mutants (Table 1) were consistent with the greater functional importance of the His residue at position 245 as the H245F enzyme is ~4-fold less active than H244F. Surprisingly, the H245A mutant had the highest specific activity of the four mutants we tested.

Integrated specific activity values for the luciferases were determined from estimates of total light output obtained by measuring the light emitted over a 15 min interval in optimized bioluminescence assays (Table 1 and Figure 3). These data varied ~40-fold. Apparently, the amino acid substitutions had a greater effect on the overall rate of light production than on the total amount of light emitted. The integrated specific activity of H245A was the highest among the mutants and was nearly equivalent to WT indicating that the imidazole functional group of His245 is not necessary to maintain an environment conducive to highly efficient radiative decay of the oxyluciferin excited state.

We undertook two additional experiments to qualitatively determine whether the altered emission time courses for the His245 mutants (Figure 3) were related to adenylate formation (Figure 1, step a) and/or utilization of oxygen (step c). When bioluminescence was initiated by injection of solutions of synthetic luciferyl−AMP, thus bypassing step a, the rise times to peak light output of WT and H245A were nearly unchanged compared to reactions initiated with luciferin and Mg-ATP (Table 1). This result indicated that the imidazole side chain is not necessary for efficient adenylate formation (Figure 1, step a). The rise times for bioluminescence reactions of H245D and H245F with synthetic luciferyl−AMP were ~6- and ~4-fold shorter, respectively, than those initiated with the natural substrates. These results with synthetic luciferyl−AMP imply that a negative charge or nonpolar aromatic ring at position 245 interferes with adenylate synthesis. The rise time for H245D with luciferyl−AMP still remained ~25 times slower than WT with the synthetic substrate, whereas the rise time of H245F was now equivalent to the WT value. These findings suggest that the carboxylate group of H245D interferes with an additional step in the bioluminescence process.

Next, the H245-substituted luciferases were each preincubated with luciferin and Mg-ATP under anaerobic conditions, thereby enabling the presumed luciferyl−AMP C-4 carbanion intermediate to form and accumulate (Figure 1, steps a and b). The addition of oxygenated buffer to an anaerobic native luciferase solution was reported (*54*) to produce a rapid flash of light with a rise time of ~0.06 s measured by stopped-flow techniques. In our trials with equipment only capable of measuring rise times of >0.3 s, the injection of O_2-saturated buffer into the anaerobic enzyme−substrate solutions produced a rapid flash of light within 0.35 ± 0.15 s for WT, H245A, and H245F. The rise time for the aspartate mutant in this experiment was 1.2 ± 0.15 s and maximal light emission was reached ~50 times faster than under the standard assay conditions (Table 1). The results of the anaerobic experiments taken together with the synthetic luciferyl−AMP trials (above) suggested that the reaction of O_2 (Figure 1, step c) with the H245 mutants does not cause the longer rise times we had observed (Table 1). It is therefore improbable that His245 is directly involved in oxygen binding, a possibility we had previously considered (*39*). DeLuca and McElroy have postulated (*54*) that a large Lase conformational change occurs prior to O_2 addition and after C-4 proton removal. The proton abstraction process (Figure 1, step b) has long been thought to be the rate-determining step in firefly bioluminescence and recent results of kinetic isotope effect studies (*9*) support this notion. It is possible that the imidazole group of His245 may assist in C-4 proton removal; however, it cannot be the Lase base directly responsible for proton abstraction. A luciferase mutant lacking this critical functional group would almost certainly be a severely impaired oxidase. Instead, the H245A and H245F mutants, both lacking a basic group at position 245, are reasonably active catalysts of bioluminescence. Possibly, a histidine at position 245 may be important to enable significant conformational movements (*54*) to proceed normally.

Table 2: Steady-State Kinetic Constants for Luciferase Enzymes[a]

enzyme	K_m (μM) luciferin	K_m (μM) Mg-ATP	k_{cat} (s^{-1})[b]
WT	15 ± 2	160 ± 20	1.6± 0.3
H245D	64 ± 5	1820 ± 40	0.0018 ± 0.0002
H245A	15 ± 2	240 ± 30	0.51 ± 0.06
H245F	89 ± 6	830 ± 30	0.045 ± 0.002

[a] Kinetic constants were determined as described in the Materials and Methods. [b] Calculated from the data used to determine the K_m values for luciferin.

Effects of His245 Substitutions on Substrate Binding and Catalytic Constants. To evaluate the effect of substitutions at His245 on the kinetic behavior of luciferase, the steady-state kinetic parameters for the WT and mutant luciferases were determined (Table 2). The K_m values for the WT enzyme were comparable to those reported for native Lase (*41, 55*). The H245D and H245F mutants exhibited increases in the K_m for luciferin of ~4- and ~6-fold, respectively, whereas the H245A value was equivalent to WT. The H245 mutants had elevated K_m values for Mg-ATP ranging from an ~1.5-fold increase for H245A to an ~12-fold increase for H245D. The effects of the changes at position 245 on k_{cat} were more pronounced than those on K_m (Table 2). All H245 mutants are catalytically compromised exhibiting k_{cat} values ~3-fold (H245A), ~36-fold (H245F), and ~900-fold (H245D) lower than WT. The kinetic results indicated that the His245 imidazole side chain is not necessary for productive luciferin binding and only has a minor role in Mg-ATP binding and catalysis of bioluminescence. However, the negative charge of a carboxylate ion (H245D) or a phenyl ring (H245F) interferes with the normal binding of both substrates probably by electrostatic repulsion and steric hindrance, respectively. The kinetic results strongly suggested that His245 is situated near the binding sites of both substrates.

A Potential Lase Active-Site Model. We undertook molecular modeling studies to produce a potential model of the Lase active site to provide a structural context for our mutational studies. Our modeling of the complex of Lase and its natural substrates was based on the work of Conti, Brick, and co-workers, who solved the Lase crystal structure without ligands (*38*) and the recently reported crystal structure of PheA complexed with Phe, AMP, and Mg ion

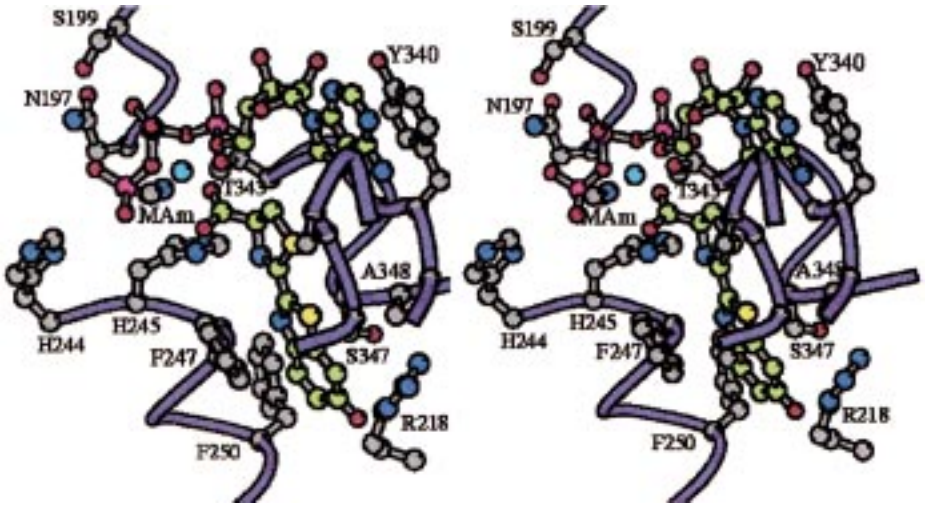

FIGURE 4: Stereo diagram showing the interactions predicted by molecular modeling of Lase with substrates luciferin and ATP (carbon atoms are green in both) and Mg^{2+} ion (cyan) with Lase. The methylammonium ion (MAm) was included to represent potential interactions of the K529 side chain. Traces through the α-carbons of regions N197−G200, H244−T252, S314−L319, and Q338−I351 are shown in purple. The α-carbons of G246, G315, G316, A317 (and side-chain methyl), G339, and G341 are shown (gray) but are not labeled. This diagram was generated using the program MOLSCRIPT (*56*).

(*40*). Lase and PheA have 550 and 556 amino acids, respectively, and share 16% sequence identity. The topology of the structural domains of the two proteins are reported to be quite similar except that the C-terminal domain of PheA is rotated 94° relative to the N-terminal domain and is 5 Å closer to it compared to the Lase structure (*40*). This distinct orientation is significant because it enables the side chain of invariant C-terminal domain residue K517 (K529 in Lase) to hydrogen bond to both Phe and AMP (*38*).

The binding geometry described in this paper is based on the lowest energy structure that was identified using the protocols described in the Materials and Methods. The structure presented here as our model (Figures 4 and 5) is only one of many low-energy binding structures and may not necessarily describe the actual binding geometry. It is, however, the lowest energy conformer of the largest family of conformations identified.

The positions of the main-chain atoms of the Lase residues in close contact with substrates in our model are very similar to the original starting crystal structure except for the loop S314−L319 (Figure 6) and the region Q338−A348. As predicted by Conti and Brick et al. (*40*), a substantial conformational change in the S314−L319 loop was required, since the peptide blocked access to the binding pockets for luciferin and the adenine ring of ATP. The S314−L319 loop and Q338−A348 region are both highly conserved among the luciferases (*20*), consistent with their important roles in substrate binding.

In our Lase model (Figures 4 and 5), the binding pocket for the adenine ring of ATP is comprised of residues 316GAP318, 339GYGL342, and V362. Amino acids in equivalent positions in PheA share similar functions. Firefly luciferin is shown in a pocket surrounded by peptides 341GLT343 and 346TSA348; helix residues 245HHGF-GMT251; and mobile loop residues 315GGA317. The side chain of R218 is situated at the bottom of the binding pocket. Many of these amino acids at equivalent positions in the adenylate-forming superfamily appear to be well-conserved (*20*−*23*, *40*) and probably have similar substrate-binding functions. It has been suggested (*38*) that residues of opposite charge at positions 250 or 286 (Lase numbering) are involved in binding-charged substrates in several peptide synthetases; e.g., a lysine residue at the 250 position may interact with the glutamate substrate of the glutamate-activating subunit of surfactin synthetase 1 (*40*). The luciferases have neutral or hydrophobic residues at these positions, and instead, the invariant guanidinium ion of R218 appears to make a favorable electrostatic interaction with the phenoxide ion of luciferin ($pK_a \approx 8.5$). According to our proposal (Figures 4 and 5), interactions with residues R218, F247, A348, H245, and K529 (methylammonium ion in our simulations) appear to fix the position of luciferin in the binding pocket. Consequently, one of the luciferin carboxylate oxygen atoms points toward the α-phosphorus atom of ATP. This arrangement may well promote the initial step in adenylate formation.

Role of 244HHGF247. Helix residues 245−247 of the Lase peptide 244HHGF247 comprise part of a binding pocket for firefly luciferin and are in close contact with the substrate (Figure 4). The substrate analogue BPTC would be expected to be similarly situated in this binding site, thereby providing a very feasible explanation for the highly efficient and specific photooxidation reaction we had previously described (*39*). Invariant F247 in the luciferases may participate in luciferin binding through a π-stacking interaction with the benzothiazole ring of the substrate (Figure 4). The imidazole side chain of invariant His245 appears to sit at the opening of the luciferin-binding pocket with its Nδ1H ∼2 Å away from a luciferin carboxylate oxygen and ∼3 Å from the nitrogen atom of the thiazoline ring. The NE2 atom of His245 is predicted to be ∼3.5 Å from the γ-phosphate of ATP. The modeled position of His245 therefore provides a structural basis for the disruptive effects on substrate binding and catalysis reported here with mutants H245D and H245F. Studies with H245A, however, indicate that maintaining the specific interactions unique to an imidazole side chain have very minor effects on substrate binding and only modest effects on light production. Apparently, a histidine at position 245 is important for the efficient formation of a luciferyl−AMP intermediate primed to react with O_2. Pos-

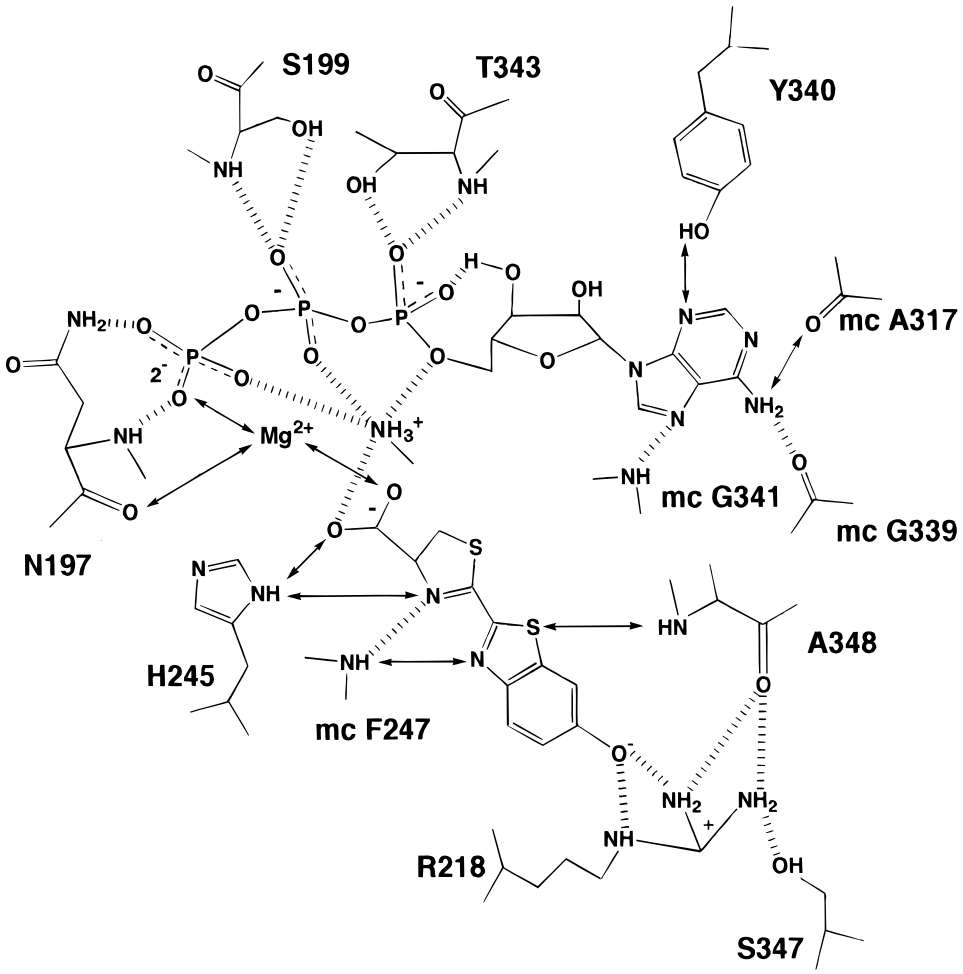

FIGURE 5: Schematic representation of hydrogen bonding (||||) between Lase and substrates luciferin, ATP and Mg^{2+} predicted by molecular modeling. Potential interactions between substrates and atoms in close proximity (~2 to ~4 Å) are indicated (↔). For main chain (mc) atoms, only those interacting with substrates are included. The methylammonium ion was used to represent possible interactions of the K529 side chain. For clarity, additional potential contacts of the Mg^{2+} ion with the T343 side chain and the O3 atoms of the α- and β-phosphates of ATP are not shown.

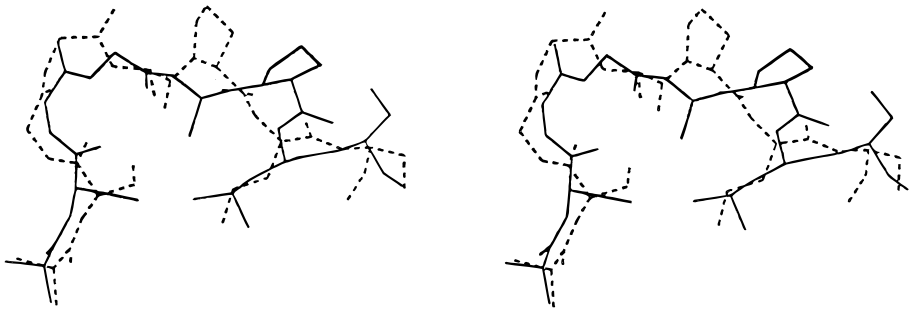

FIGURE 6: Stereo diagram of the superimposed Lase regions 313ASGGAPLS320 from the X-ray structure (- - -) (*38*) and the molecular model (—). This diagram was generated using the program MOLSCRIPT (*56*).

sibly, His245 assists in positioning luciferyl−AMP for this transformation.

Concluding Remarks. The results of mutational, biochemical, and molecular modeling studies reported here have enabled us to offer a structure-based explanation for the BPTC-catalyzed photoinactivation of Lase. In turn, we have described the possible function of the photooxidized Lase peptide 244HHGF247 based on our model. All of the His245 mutants reported (Table 1) here and additional ones we are currently studying display red-shifted bioluminescence emission spectra. A study is currently in progress to investigate the possible role of His245 in determining the color of bioluminescence. We expect that the results of our ongoing study and those of others will be better understood in light of the significant detail our model has added to the X-ray structure of Lase (*38*).

ACKNOWLEDGMENT

We thank Monika Gruber and Justin Stroh for helpful discussions; David Lloyd, John Thompson, and the DNA Sequencing Facility, Pfizer Inc., for providing the DNA sequencing data; Boris Chrunyk for assistance with the circular dichroism studies; and Jud Grice and Evelyn Bamford for technical assistance.

REFERENCES

1. Lloyd, J. E. (1978) in *Bioluminescence in Action* (Herring, P. J., Ed.) pp 241−272, Academic Press, New York.
2. Hastings, J. W. (1995) in *Cell Physiology Source Book* (Sperelakis, N., Ed.) pp 665−681, Academic Press, New York.
3. DeLuca, M. (1976) *Adv. Enzymol. 44*, 37−68.
4. Seliger, H. H., and McElroy, W. D. (1960) *Arch. Biochem. Biophys. 88*, 136−141.
5. White, E. H., Rapaport, E., Seliger, H. H., and McElroy, W. D. (1971) *Bioorg. Chem. 1*, 92−122.
6. White, E. H., Steinmetz, M. G., Miano, J. D., Wildes, P. D., and Morland, R. (1980) *J. Am. Chem. Soc. 102*, 3199−3208.
7. McElroy, W. D., and Seliger, H. H. (1966) in *Molecular Architecture in Cell Physiology* (Hayashi, H., and Szent-Gyorgyi, I., Eds.) pp 63−79, Prentice-Hall, Englewood Cliffs, NJ.
8. Hastings, J. W. (1996) *Gene 173*, 5−11.
9. McCapra, F., Gilfoyle, D. J., Young, D. W., Church, N. J., and Spencer, P. (1994) in *Bioluminescence and Chemiluminescence: Fundamentals and Applied Aspects* (Campbell, A. K., Kricka, L. J., and Stanley, P. E., Eds.) pp 387−391, John Wiley & Sons, Chichester.
10. McCapra, F. (1997) in *Bioluminescence and Chemiluminescence: Molecular Reporting with Photons* (Hastings, J. W., Kricka, L. J., and Stanley, P. E., Eds.) pp 7−15, John Wiley & Sons, Chichester.
11. Wood, K. V. (1995) *Photochem. Photobiol. 62*, 662−673.
12. Fontes, R., Dukhovich, A., Sillero, A., and Günther-Sillero, M. A. (1997) *Biochem. Biophys. Res. Commun. 237*, 445−450.
13. Ortiz, B., Fernandez, V. M., Günther-Sillero, M. A., and Sillero, A. (1995*) J. Photochem. Photobiol. B. Biol. 29*, 33−36.
14. Kricka, L. J. (1988) *Anal. Biochem. 175*, 14−21.
15. Campbell, A. K., and Sala-Newby, G. B. (1993) in *Fluorescent and Luminescent Probes for Biological Activity* (Mason, W. T., Ed.) pp 58−82, Academic Press, London.
16. Kricka, L. J. (1995) *Anal. Chem. 67*, 499R−502R.
17. deWet, J. R., Wood, K. V., DeLuca, M., Helinski, D. R., and Subramani, S. (1987) *Mol. Cell. Biol. 7*, 725−737.
18. Gould, S. J., and Subramani, S. (1988) *Anal. Biochem. 175*, 5−13.
19. Contag, C. H., Spilman, S. D., Contag, P. R., Oshiro, M., Eames, B., Dennery, P., Stevenson, D. K., and Benaron, D. A. (1997) *Photochem. Photobiol. 66*, 523−531.
20. Ye, L., Buck, L. M., Schaeffer, H. J., and Leach, F. R. (1997) *Biochim. Biophys. Acta 1339*, 39−52.
21. Suzuki, H., Kawarabayasi, Y., Kondo, J., Abe, T., Nishikawa, K., Kimura, S., Hashimoto, T., and Yamamoto, T. (1990) *J. Biol. Chem. 265*, 8681−8685.
22. Babbitt, P. C., Kenyon, G. L., Martin, B. M., Charest, H., Sylvestre, M., Scholten, J. D., Chang, K.-H., Liang, P.-H., and Dunaway-Mariano, D. (1992) *Biochemistry 31*, 5594−5604.
23. Chang, K.-H., Xiang, H., and Dunaway-Mariano, D. (1997) *Biochemistry 36*, 15650−15659.
24. Sala-Newby, G. B., and Campbell, A. K. (1991) *Biochem. J. 279*, 727−732.
25. Kajiyama, N., and Nakano, E. (1991) *Protein Eng. 4*, 691−693.
26. Ohmiya, Y., Hirano, T., and Ohashi, M. (1996) *FEBS Lett. 384*, 83−86.
27. Mamaev, S. V., Laikhter, A. L., Arslan, T., and Hecht, S. M. (1996) *J. Am. Chem. Soc. 118*, 7243−7244.
28. Arslan, T., Mamaev, S. V., Mamaeva, N. V., and Hecht, S. M. (1997) *J. Am. Chem. Soc. 119*, 10877−10887.
29. Wood, K. V., Lam, Y. A., Seliger, H. H., and McElroy, W. D. (1989) *Science 244*, 700−702.
30. Alter, S. C., and DeLuca, M. (1986) *Biochemistry 25*, 1599−1605.
31. Vellom, D. C. (1990) Ph.D. Dissertation, University of California, San Diego.
32. Dementieva, E. I., Zheleznova, E. E., Kutuzova, G. D., Lundovskikh, I. A., and Ugarova, N. N. (1996) *Biochemistry (Moscow) 61*, 115−119.
33. Branchini, B. R., Magyar, R. A., Murtiashaw, M. H., Magnasco, N., Hinz, L. K., and Stroh, J. G. (1997) *Arch. Biochem. Biophys. 340*, 52−58.
34. Ohmiya, Y., and Tsuji, F. I. (1997) *FEBS Lett. 404*, 115−117.
35. Kajiyama, N., and Nakano, E. (1993) *Biochemistry 32*, 13795−13799.
36. White, P. J., Squirrell, D. J., Arnaud, P., Lowe, C. R., and Murray, J. A. H. (1996) *Biochem. J. 319*, 343−350.
37. Thompson, J. F., Geoghegan, K. F., Lloyd, D. B., Lanzetti, A. J., Magyar, R. A., Anderson, S. M., and Branchini, B. R. (1997) *J. Biol. Chem. 272*, 18766−18771.
38. Conti, E., Franks, N. P., and Brick, P. (1996) *Structure 4*, 287−298.
39. Branchini, B. R., Magyar, R. A., Marcantonio, K. M., Newberry, K. J., Stroh, J. G., Hinz, L. K., and Murtiashaw, M. H. (1997) *J. Biol. Chem. 272*, 19359−19364.
40. Conti, E., Stachelhaus, T., Marahiel, M. A., and Brick, P. (1997) *EMBO J. 16*, 4174−4183.
41. Branchini, B. R., Hayward M. M., Bamford, S., Brennan P. M., and Lajiness, E. J. (1989) *Photochem. Photobiol. 49*, 689−695.
42. Zoller, M. J., and Smith, M. (1983) *Methods Enzymol. 100*, 468−500.
43. Green, A. A., and McElroy, W. D. (1956) *Biochim. Biophys. Acta 20*, 170−176.
44. Laemmli, U. K. (1970) *Nature 227*, 680−685.
45. Herbst, R., Schäfer, U., and Seckler, R. (1997) *J. Biol. Chem. 272*, 7099−7105.
46. Mohamadi, F., Richards, N. G. F., Guida, W.C., Liskamp, R., Lipton, M., Caulfield C., Chang, G., Hendrickson T., and Still, W. C. (1990) *J. Comput. Chem. 11*, 440−467.
47. Ferguson, D. M., and Kollman, P. A. (1991) *J. Comput. Chem. 12*, 620−626.
48. McDonald, Q., and Still, W. C. (1992) *Tetrahedron Lett. 33*, 7743−7746.
49. Bernstein, F. C., Koetzle, T. F., Williams, J. G. B., Meyer, E. F., Brice, M. R., Rodgers, J. R., Kennard, O., Shimanouchi, T., and Tasumi, M. (1977) *J. Mol. Biol. 122*, 535−542.
50. Chang, G., Guida, W. C., and Still, W. C. (1989) *J. Am. Chem. Soc. 11*, 4379−4386.
51. Saunders, M., Houk, K. N., Wu, Y.-D., Still, W. C., Lipton, M., Chang, G., and Guida, W. C. (1990) *J. Am. Chem. Soc. 112*, 1419−1427.
52. Shenkin, P. S., and McDonald, D. Q. (1994) *J. Comput. Chem. 15*, 899−916.
53. Amburgey, J. C., Shuey, S. W., Pedersen, L. G., and Hiskey, R. G. (1994) *Biorg. Chem. 22*, 172−197.
54. DeLuca, M., and McElroy, W. D. (1974) *Biochemistry 13*, 921−925.
55. DeLuca, M., and McElroy, W. D. (1984) *Biochem. Biophys. Res. Commun. 123*, 764−770.
56. Kraulis, P. J. (1991) *J. Appl. Crystallogr. 24*, 946−950.

BI981150D